



# HHS Public Access

Author manuscript

*Pediatr Cardiol.* Author manuscript; available in PMC 2022 October 19.

Published in final edited form as:

*Pediatr Cardiol.* 2019 January ; 40(1): 79–88. doi:10.1007/s00246-018-1963-z.

## Improved Workflow for Quantification of Right Ventricular Volumes Using Free-Breathing Motion Corrected Cine Imaging

Anthony Merlocco<sup>1,3</sup>, Laura Olivieri<sup>1</sup>, Peter Kellman<sup>2</sup>, Hui Xue<sup>2</sup>, Russell Cross<sup>1</sup>

<sup>1</sup>Division of Cardiology, Children's National Health System, and the Department of Pediatrics, George Washington Medical School, Washington, DC, USA

<sup>2</sup>National Institutes of Health/NHLBI, 10 Center Dr., Bethesda, MD, USA

<sup>3</sup>University of Tennessee Health Science Center, Le Bonheur Children's Hospital, 49 N. Dunlap Room 363, Memphis, TN 38103, USA

### Abstract

Cardiac MR traditionally requires breath-holding for cine imaging. Younger or less stable patients benefit from free-breathing during cardiac MR but current free-breathing cine images can be spatially blurred. Motion corrected re-binning (MOC) is a novel approach that acquires and then reformats real-time images over multiple cardiac cycles with high spatial resolution. The technique was previously limited by reconstruction time but distributed computing has reduced these times. Using this technique, left ventricular volumetry has compared favorably to breath-held balanced steady-state free precession cine imaging (BH), the current gold-standard, however, right ventricular volumetry validation remains incomplete, limiting the applicability of MOC in clinical practice. Fifty subjects underwent cardiac MR for evaluation of right ventricular size and function by end-diastolic (EDV) and end-systolic (ESV) volumetry. Measurements using MOC were compared to those using BH. Pearson correlation coefficients and Bland–Altman plots tested agreement across techniques. Total scan plus reconstruction times were tested for significant differences using paired *t*-test. Volumes obtained by MOC compared favorably to BH ( $R = 0.9911$  for EDV,  $0.9690$  for ESV). Combined acquisition and reconstruction time (previously reported) were reduced 37% for MOC, requiring a mean of 5.2 min compared to 8.2 min for BH ( $p < 0.0001$ ). Right ventricular volumetry compares favorably to BH using MOC image reconstruction, but is obtained in a fraction of the time. Combined with previous validation of its use for the left ventricle, this novel method now offers an alternative imaging approach in appropriate clinical settings.

---

<sup>✉</sup> Anthony Merlocco, amerlocc@uthsc.edu.

**Conflict of interest** Anthony Merlocco, Laura Olivieri, Peter Kellman, Hui Xue and Russell Cross declares that they have no conflict of interest.

**Ethical Approval** All procedures performed in studies involving human participants were in accordance with the ethical standards of the Institutional Review Board of Children's National Health System and with the 1964 Helsinki declaration and its later amendments or comparable ethical standards.

**Informed Consent** Written informed consent, and assent when appropriate, was obtained from all study participants.

## Keywords

Retrospective reconstruction; Cardiac volume; Motion correction; Cardiovascular MR; Free-breathing; Reconstruction time

---

## Introduction

Expedient and accurate assessment of cardiac volume and function remains a strength of cardiovascular magnetic resonance imaging (CMR) in pediatric patients. Accurate and reproducible assessment of cardiovascular structure and function by CMR is currently relatively straightforward in both adult and pediatric patients who can reliably hold their breath [1, 2]. However, in pediatric patients both clinical and patient factors frequently limit or prohibit breath-holding. Highly reproducible, reliable, accurate, and time-efficient free-breathing imaging would allow extension of cardiac MR assessment to a younger population that cannot reliably follow instruction or a sick population in whom breath-holding is not practical. Imaging the cardiovascular system is complex, requiring strategies to limit the effect of both cardiac and respiratory motion. Traditionally this has been accomplished using cardiac gating to account for cardiac motion and using a breath-hold to limit respiratory motion. “Cine” imaging, typically performed using balanced steady-state free precession (bSSFP) sequences, images the heart multiple times per cardiac cycle by collecting multiple segments per heartbeat, which are then reconstructed to display a determined number of frames per heartbeat, which is generally 30 reconstructed frames [3, 4]. Breath-held bSSFP (BH) cardiac MR imaging provides high spatial and temporal resolution, permitting clear definition of the interface between blood and myocardium throughout the cardiac cycle, which is imperative to collecting images at peak systole and end-diastole [5–9]. Collection of this data without requiring a breath-hold in cases of young, cognitively limited, ill, or fatigued patients is difficult. Alternative approaches with free-breathing have been limited in providing similar spatial and temporal resolution to the gold-standard of BH. In order to be integrated clinically, a free-breathing sequence must be robust in its agreement with BH for volume and function assessment and require similar imaging time. Importantly, for evaluation of the left ventricle, our group has shown a novel method, motion corrected retrospective re-binning, provides accurate and reproducible ventricular volume and function assessment, however, this cannot simply be extrapolated to the right ventricle as right ventricular shape and thickness differs from the left ventricle and is not subject to identical hemodynamic effects when free-breathing [10].

The basis of motion corrected retrospective re-binning evolved from early signal-average techniques, which have been applied to free-breathing patients, but the associated respiratory averaging often results in blurring, thus limiting quantitative assessment [2]. Real-time cine via single shot acquisition produces images unaffected by respiratory motion but with limited spatial resolution [11–13]. Kuhl et al. compared image quality and wall motion scoring in two real-time cardiac MR sequences to BH and demonstrated that wall motion scoring of real-time radial bSSFP imaging was similar to imaging acquired with breath-holding with Cohen kappa coefficients for agreement of 0.89 [11]. Further, Lee et al. studied twelve healthy volunteers and eight patients with cardiac disease to compare realtime

true fast imaging with steady-state precession (FISP) to BH and found measurements of resting left ventricular function were comparable [12]. However, real-time imaging requires high parallel imaging factors, resulting in signal-to-noise loss, which can be mitigated to some degree by multiple averages and utilization of motion correction. Improvement in signal-to-noise ratio and the temporal resolution remains important however, and thus our study's novel re-binning technique was developed wherein a real-time sequence collects and time-stamps raw data at a high spatial resolution with parallel imaging, then retrospectively reconstructs to a higher temporal resolution following respiratory motion correction and re-binning of data over multiple heartbeats [14]. Signal-to-noise and temporal resolution with the novel re-binning imaging technique is improved compared to real-time imaging and can be performed with non-Cartesian protocols [15]. Until recently, the clinical utility of motion corrected re-binning was limited not by its acquisition time or image quality but by the computational delay to completing the image reconstruction, which required 1–2 min per slice, resulting in up to 15 min for acquisition and reconstruction of a short-axis stack [13]. Previously, an open-source framework for medical image reconstruction has been developed, which allows raw data marked with a message ID, to be deserialized and passed through a series of processing modules. The system, termed the “Gadgetron,” returns images or partially processed data which can then be reconstructed to sequential images based on the message ID [16]. Distributed computing, wherein multiple “nodes” are employed to disperse the required computations, has greatly reduced reconstruction times and can be decentralized through a cloud-based service, with resultant total imaging and reconstruction times on the order of 5 min [10, 16].

Full clinical integration of this important and novel technique requires verification of reliable and accurate function and volume assessment of both ventricles. While the results for left ventricular assessment with motion corrected re-binning were encouraging, the right ventricular wall appearance and physiology differ from that of the left ventricle. Through comparison of motion corrected re-binning (MOC) to BH for right ventricular volumetry, we aim to demonstrate that while the right ventricular shape and thickness differs from the left ventricle, the volumetric assessment via motion corrected retrospective re-binning will compare favorably to the clinically standard BH, allowing forward progress with this valuable and innovative method of cardiac assessment.

## Methods

The study dataset was composed of subjects recruited for creation of a pool of normal studies to be used for longitudinal technical development testing. The dataset includes both patients who presented clinically for a CMR scan as well as volunteers. All patients and volunteers were considered for dataset inclusion if their CMR results were found to be normal, resulting in 25 healthy volunteers and 25 patients. Written informed consent, and assent when appropriate, was obtained from all study participants. The Institutional Review Board of Children's National Health System approved the technical development protocol establishing dataset creation. All study participants underwent BH and MOC imaging and were only included if a full dataset could be collected. This dataset was previously reviewed by Cross et al. [10] for assessment of LV volumetry. Subjects were scanned using a 1.5T MR scanner (MAGNETOM Aera, Siemens Healthcare, Erlangen, Germany) with an 18-channel

body matrix array anteriorly and a spine array posteriorly. Breath-hold instructions were reviewed prior to and during the scan for end-expiration imaging. Image reconstruction of MOC images was performed online using the Gadgetron as previously described [10, 16].

### Imaging Sequences

Imaging parameters were standardized and one of three existing protocols utilized by our CMR laboratory was used: infant, child, or teenager. Typical imaging parameters have been described previously [10] and are reviewed in Table 1.

Mechanical ventilation was utilized in clinically-indicated CMR for infants and children. BH cine imaging acquisition was performed using one breath-hold per slice, 8–12 s per slice with a 10–15 s rest period. For BH imaging, ventilation pauses, acquisition times, and rest times were kept similar to that as in conscious subjects. MOC imaging was completed without specific breathing instruction, allowing spontaneous breathing, unless subjects were under anesthesia for clinical reasons, in which case the ventilator-determined rate was utilized. The right ventricle was imaged in short-axis with coverage from the apex to the outflow tract with 30 reconstructed phases through the cardiac cycle. BH and MOC image position and image orientation did not differ within each individual patient's scan.

As the scans themselves were the same as those analyzed by Cross et al. for the left ventricle, total imaging time for each sequence type has been previously reported but bears reiteration. Total scan time was determined by time from sequence initiation to complete image reconstruction and display on the workstation, thus including all time required for acquisition, rest breaks during BH sequences, and reconstruction [10].

### Image Reconstruction

Gadgetron distributed framework was used for MOC image reconstruction. Gadgetron is an open-source reconstruction framework, which has been extended with new software components that enable a cloud-based distributed deployment and integration with the scanner for stream-lined processing [17]. Images were returned to the scanner immediately after reconstruction with no user interaction. Distributed computing strategies included multiple nodes deployed through Amazon EC2, or several local nodes in combination, with similar reconstruction times through any given deployment [10].

### Right Ventricular Function and Quantification

QMass software (Medis Medical Imaging Systems, Leiden, The Netherlands) was used for post-processing of right ventricular volumes after all images had been anonymized prior to transfer from the scanner. Summation of disks was used to determine RV volume and function after tracing of endocardium in end-diastole (EDV) and end-systole (ESV). Two observers with 2 and 9 years of CMR experience (AM and LO) independently performed endocardial tracings.

## Statistical Analyses

MOC acquisition was measured against BH acquisition by correlation analysis for predictability assessment with significance of  $p < 0.05$  as threshold for rejection of non-linearity.

Additionally, the degree of linear correlation was assessed by Pearson correlation coefficients. Measurement bias and limits of agreement (95% as  $\pm 1.96$  SD) were determined with Bland–Altman plots [18]. Inter-observer agreement between AM and LO was expressed by concordance correlation coefficient and through Bland–Altman plots [19, 20]. As previously reported by Cross et al. [10], the scan and reconstruction times were expressed as mean  $\pm$  SD, and techniques were compared with a paired  $t$ -test. MedCalc was used for all statistical analysis 0 (MedCalc Software, v.12.2.1.0 Ostend, Belgium).

## Results

### Subjects

Our research database yielded 25 patients and 25 volunteers  $21.6 \pm 11.4$  years old (2.1–56.6) [mean  $\pm$  SD (range)] who underwent both BH and MOC imaging during the same CMR study resulting in analyzable data. The study population included seven children below the age of 13 years (14%), one of whom was an infant. Weight [ $57.5 \pm 26.9$  kg (2.3–101)] and body surface area [ $1.6 \pm 0.4$  m<sup>2</sup> (0.4–2.2)] reflect these demographics. Sixty-two percent were female. Average heart rate was  $67 \pm 11.5$  bpm (46–100) for BH imaging and was  $71 \pm 11.6$  bpm (46–100) for MOC imaging. Illustrative slices from the papillary muscle level are shown in Fig. 1 for end-diastole and end-systole from one subject with endocardial tracing. All RV EDV and ESV measurements for both imaging techniques obtained by primary observer are reported in Fig. 2. EDV and ESV sample means for BH and MOC imaging demonstrate satisfactory agreement with an observed trend to overestimation of ESV for MOC compared with BH. Pearson correlation is reported in Fig. 3 for volume quantification of MOC imaging compared with BH. Correlation between MOC and BH is excellent for each measure assessed with Pearson correlation for MOC EDV of  $R = 0.9911$  and for ESV of  $R = 0.9690$  compared to BH (both  $p < 0.0001$ ) (Fig. 3).

Agreement of right ventricular volume quantification between MOC and BH acquisitions was quantified using Bland–Altman plots (Fig. 4), which plotted the differences in measurement against the gold-standard BH measurements, demonstrating acceptable performance of the MOC acquisition for EDV measurements, with minimal mean bias difference compared to BH (mean bias + 0.9 ml). ESV measurement agreement demonstrated minimal bias (mean bias – 3.3 ml for MOC).

### Inter-observer Reproducibility

Agreement for right ventricular volume quantification between observers was quantified using Bland–Altman plots (Fig. 5) of EDV and ESV. In addition, Pearson correlation analysis was performed, demonstrating a strong linear relationship between the measurements ( $R = 0.9786$  comparing BH EDV measurements; 0.9804 for MOC EDV measurements; 0.9572 for BH ESV measurements; and 0.9665 for MOC ESV

measurements) (Fig. 6). Concordance correlation coefficients and Bland–Altman analysis comparing EDV and ESV measurements for inter-observer variability are summarized in Table 2. The two observers demonstrate minimal mean bias for MOC and for BH in EDV and ESV measurement. The McBride scale was used and demonstrated substantial strength of agreement for BH EDV between observers ( $\rho_c$  0.95–0.99) and moderate strength for BH and MOC ESV and MOC EDV ( $\rho_c$  0.90–0.95) [19].

### Image Acquisition and Reconstruction Time

Total image data acquisition and reconstruction times have been previously reported in our earlier study for left ventricular MOC volumetry assessment using the same technical development dataset [10]. To reiterate, the mean combined total acquisition and reconstruction times for MOC is shorter than standard BH techniques, requiring a mean of 5.2 min compared to 8.2 min, resulting in a total imaging time reduction of 37% ( $p < 0.0001$ ) (Fig. 7).

### Discussion

This study sought to demonstrate the ability of motion corrected re-binning image reconstruction to quantify right ventricular volume as compared to the gold-standard of BH imaging in both pediatric and adult subjects. While previous work has demonstrated MOC evaluation of the left ventricle produces reliable and accurate functional measurements, which can be performed quickly using cloud-based image reconstruction [10], a complete CMR study includes right ventricular volumetry and we have now shown that MOC imaging of the right ventricle compares favorably to the gold-standard BH imaging with similar calculated EDV and ESV. For the previous left ventricular assessment, analysis included contextualization of the bias results from the Bland–Altman plots using published data from Suinesiaputra et al. who described biases of LV EDV and ESV on 15 identical image data sets and we achieved very similar results [7, 10]; an equivalent right ventricular analysis has not been published. For some context, however, we can compare our RV biases to our LV biases and they are of a relatively similar scale with RV EDV average bias + 0.9 ml compared to LV EDV of 1.1 ml; RV ESV of – 3.3 ml compared to LV ESV of 5.7 ml [10]. As with the LV volumetry study, there is a tendency for MOC to overestimate the ESV compared to the BH technique, which was present in both independent observers. As previously, we hypothesize that this is likely due to endocardial blurring resulting from in-plane motion that is exaggerated by signal averaging in both methods.

Inter-observer reproducibility of right ventricular volumetry demonstrates modest agreement. However, the inter-observer variability for both BH and MOC in our study compares well with a study of CMR measurement reproducibility in normal right ventricles that reported mean differences for RV EDV measurement of 12.7 ml with 95% CI between – 10.5 and 35.9 ml and for RV ESV of 8.4 ml with 95% CI between – 15.2 and 31.9 ml [21].

Given the meager reproducibility of right ventricular mass measurement, both compared to left ventricular measurement and in its own right [21–25], our laboratory does not report right ventricular end-diastolic mass clinically. In light of the lack of agreement regarding the validity of measuring right ventricular mass, we did not assess it in this study.

While traditional BH volumetric imaging remains our laboratory's clinical standard for daily use, the MOC technique has provided great advantage in pediatric patients. Often this age-group has difficulty with prolonged or repetitive breath-holds and may not understand the instructions. As well, frequent pausing of aids like music or movie projection has resulted in frustration or greater awareness of the scan duration in our younger patients, which has been ameliorated using MOC. Because we now have shown that MOC yields comparable EDV and ESV results to BH imaging for both ventricles in a fraction of the time, we have been able to integrate the MOC technique clinically with minimal concern for accuracy of volumetry of either ventricle. As well, patients from our cardiac patient ward and intensive care unit frequently require functional assessment that we may now provide to those too ill to complete a breath-hold yet not unstable enough to require mechanical ventilation. MOC has few downsides, with subtle blurring and the requirement for access to cloud based reconstruction being the only notable ones. While the images acquired are not indistinguishable from those acquired by BH, the image quality remains excellent and clearly does not compromise analysis. Regarding cloud based reconstructions, as noted in our previous study, total reconstruction time for MOC is on the order of 1 min per slice [13] and previously we tested both cloud-based and locally deployed hardware for reconstruction [10]. Cloud based reconstruction can be completed through a 1 GB/s internet connection, without up-front cost and can be deployed on demand [10]. Recently we have preferred this method to locally deployed reconstruction for speed and decreased hardware maintenance requirements. Adding MOC imaging to our clinical arsenal has proved extremely valuable.

While anesthesia use in pediatric imaging is sometimes a necessity, it also may carry risk. Animal studies initially demonstrated initial and long-term functional effects after general anesthesia [26]. Particular interest has arisen in neurodevelopmental outcomes in children exposed to anesthesia with several studies underway to elucidate the effects of single anesthetic exposure, multiple exposure, and prolonged exposure [27]. With increasing awareness of possible risks as well as knowledge of exposure factors that may impact negative effects, it is prudent to continue efforts to limit anesthesia when and if possible. Our study will not only decrease requirement for general anesthesia in patients who can be studied while conscious or under light sedation but also provides the clinician with a further strategy to decrease scan time and thus anesthetic exposure in cases where general anesthesia is still used.

### Study Limitations

In this study, we intentionally included clinical patients, providing a range of subject size and imaging parameters in order to compare typical pediatric and adult congenital cardiac MR studies. This resulted in a small number of subjects imaged with the infant and pediatric imaging parameters and limits the ability to perform meaningful statistical analysis of this variation. Additionally, we found a difference in inter-observer reproducibility and this may be affected by the relative experience levels in the observers in the current study, which were 2 and 9 years at time of analysis. However, it is encouraging that MOC evaluation of the right ventricle performs similarly as that of the left ventricle. While the measurements have compared favorably, measurements obtained by the gold-standard BH technique remain the basis for volumetric data used to make prognostic determinations in clinical algorithms.

As well, while MOC imaging should be less sensitive to arrhythmia than segmented BH imaging, we did not study this specifically as our goal was to have complete datasets from both BH and MOC imaging; thus patients for whom arrhythmia limited BH imaging were excluded. Further study should include subjects with arrhythmia and subjects with dysfunction in order to determine the applicability in these populations.

## Conclusion

Right ventricular volumetry compares favorably to BH using MOC image reconstruction but is obtained in a fraction of the time. Combined with previous validation of its use for the left ventricle, this novel method now offers an alternative imaging approach in appropriate clinical settings. Motion corrected re-binning image reconstruction can provide robust and expedient cardiac imaging for a complete cardiac MR study, resulting in comparable left and right ventricular volumes to BH imaging.

## Acknowledgements

The authors wish to thank Michael Hansen PhD for his work through the National Institutes of Health/NHLBI. The combined contributions through development and implementation of the motion-corrected free-breathing re-binning technique made this work possible.

## Funding

This study was funded by the Intramural Research Program of the National Institutes of Health (US), National Heart, Lung, and Blood Institute.

## References

1. Hundley WG, Bluemke DA, Finn JP et al. (2010) ACCF/ACR/AHA/NASCI/SCMR 2010 expert consensus document on cardiovascular magnetic resonance. A report of the American College of Cardiology Foundation Task Force on Expert Consensus Documents. *J Am Coll Cardiol* 55(23):2614–2662. 10.1016/j.jacc.2009.11.011 [PubMed: 20513610]
2. Fratz S, Chung T, Greil GF et al. (2013) Guidelines and protocols for cardiovascular magnetic resonance in children and adults with congenital heart disease: SCMR expert consensus group on congenital heart disease. *J Cardiovasc Magn Reson* 15(1):51. 10.1186/1532-429X-15-51 [PubMed: 23763839]
3. Scheffler KLS (2003) Principles and applications of balanced SSFP techniques. *Eur Radiol* 13:2409–2418 [PubMed: 12928954]
4. Ridgway JP (2010) Cardiovascular magnetic resonance physics for clinicians: part I. *J Cardiovasc Magn Reson* 12(1):71. 10.1186/1532-429X-12-71 [PubMed: 21118531]
5. Maceira A, Prasad S, Khan MPD (2006) Normalized left ventricular systolic and diastolic function by steady state free precession cardiovascular magnetic resonance. *J Cardiovasc Magn Reson* 8:417–426 [PubMed: 16755827]
6. Kondo C, Caputo GR, Semelka R, Foster E, Shimakawa A, Higgins CB (1991) Right and left ventricular stroke volume measurements with velocity-encoded cine MR imaging: in vitro and in vivo validation. *Am J Roentgenol* 157(1):9–16. 10.2214/ajr.157.1.2048544 [PubMed: 2048544]
7. Suinesiaputra A, Bluemke DA, Cowan BR et al. (2015) Quantification of LV function and mass by cardiovascular magnetic resonance: multi-center variability and consensus contours. *J Cardiovasc Magn Reson* 17(1):63. 10.1186/s12968-015-0170-9 [PubMed: 26215273]
8. Pattynama PM, Lamb HJ, van der Velde EA, van der Wall EE, de Ross A (1993) Left ventricular measurements with cine and spin-echo MR imaging: a study of reproducibility with variance component analysis. *Radiology* 187:261–268 [PubMed: 8451425]



9. Grothues F, Smith GC, Moon JC et al. (2002) Comparison of interstudy reproducibility of cardiovascular magnetic resonance with two-dimensional echocardiography in normal subjects and in patients with heart failure or left ventricular hypertrophy. *Am J Cardiol* 90(1):29–34. 10.1016/S0002-9149(02)02381-0 [PubMed: 12088775]
10. Cross R, Olivieri L, O'Brien K, Kellman P, Xue H, Hansen M (2016) Improved workflow for quantification of left ventricular volumes and mass using free-breathing motion corrected cine imaging. *J Cardiovasc Magn Reson* 18(1):10. 10.1186/s12968-016-0231-8 [PubMed: 26915830]
11. Kühl HP, Spuentrup E, Wall A, Franke A, Schröder J, Heussen N, Hanrath P, Gunther RBA (2004) Assessment of myocardial function with interactive non-breath-hold realtime MR imaging: comparison with echocardiography and breath-hold cine MR imaging. *Radiology* 231(1):198–207 [PubMed: 14990805]
12. Lee VS, Resnick D, Bundy JM, Simonetti OP, Lee PWJ (2002) Cardiac function: MR evaluation in one breath hold with real-time true fast imaging with steady-state precession. *Radiology* 222:835–842 [PubMed: 11867810]
13. Xue H, Kellman P, LaRocca G, Arai AE, Hansen MS (2013) High spatial and temporal resolution retrospective cine cardiovascular magnetic resonance from shortened free breathing real-time acquisitions. *J Cardiovasc Magn Reson* 15(1):102. 10.1186/1532-429X-15-102 [PubMed: 24228930]
14. Kellman P, Ched'hotel C, Lorenz CH, Mancini C, Arai AE, McVeigh ER (2009) High spatial and temporal resolution cardiac cine MRI from retrospective reconstruction of data acquired in real time using motion correction and resorting. *Magn Reson Med* 62(6):1557–1564. 10.1002/mrm.22153 [PubMed: 19780155]
15. Hansen MS, Sørensen TS, Arai AE, Kellman P (2012) Retrospective reconstruction of high temporal resolution cine images from real-time MRI using iterative motion correction. *Magn Reson Med* 68(3):741–750. 10.1002/mrm.23284 [PubMed: 22190255]
16. Hansen M, Sørensen T (2013) Gadgetron: an open source framework for medical image reconstruction. *Magn Reson Med* 69:1768–1776 [PubMed: 22791598]
17. Xue H, Inati S, Sørensen TS, Kellman PHM (2015) Distributed MRI reconstruction using Gadgetron-based cloud computing. *Magn Reson Med* 73:1015–1025 [PubMed: 24687458]
18. Bland JMAD (1999) Measuring agreement in method comparison studies. *Stat Methods Med Res* 8:135–160 [PubMed: 10501650]
19. McBride G (2005) A proposal for strength-of-agreement criteria for Lin's concordance correlation coefficient. In: NIWA Client Report: HAM 2005-06. Report to Ministry of Health, p 6
20. Lin L (1989) A concordance correlation coefficient to evaluate reproducibility. *Biometrics* 45:255–268 [PubMed: 2720055]
21. Mooij CF, de Wit CJ, Graham DA, Powell AJ, Geva T (2008) Reproducibility of MRI measurements of right ventricular size and function in patients with normal and dilated ventricles. *J Magn Reson Imaging* 28(1):67–73. 10.1002/jmri.21407 [PubMed: 18581357]
22. Grothues F, Moon JC, Bellenger NG, Smith GS, Klein HU, Pennell DJ (2004) Interstudy reproducibility of right ventricular volumes, function, and mass with cardiovascular magnetic resonance. *Am Heart J* 147(2):218–223. 10.1016/j.ahj.2003.10.005 [PubMed: 14760316]
23. Blalock SE, Banka P, Geva T, Powell AJ, Zhou J, Prakash A (2013) Interstudy variability in cardiac magnetic resonance imaging measurements of ventricular volume, mass, and ejection fraction in repaired tetralogy of Fallot: a prospective observational study. *J Magn Reson Imaging* 38(4):829–835. 10.1002/jmri.24050 [PubMed: 23418153]
24. Caudron J, Fares J, Lefebvre V, Vivier P-H, Petitjean C, Dacher J-N (2012) Cardiac MRI assessment of right ventricular function in acquired heart disease: factors of variability. *Acad Radiol* 19(8):991–1002. 10.1016/j.acra.2012.03.022 [PubMed: 22608861]
25. Altmayer SPL, Teeuwen LA, Gorman RC, Han Y (2015) RV mass measurement at end-systole: improved accuracy, reproducibility, and reduced segmentation time. *J Magn Reson Imaging* 42(5):1291–1296. 10.1002/jmri.24899 [PubMed: 25826694]
26. Sanders RD, Hassell J, Davidson AJ, Robertson NJ, Ma D (2013) Impact of anaesthetics and surgery on neurodevelopment: an update. *Br J Anaesth* 110:i53–i72. 10.1093/bja/aet054 [PubMed: 23542078]

27. Pinyavat T, Warner DO, Flick RP et al. (2016) Summary of the update session on clinical neurotoxicity studies. *J Neurosurg Anesthesiol* 28(4):356–360. 10.1097/ANA.0000000000000347 [PubMed: 27768673]

Author Manuscript

Author Manuscript

Author Manuscript

Author Manuscript

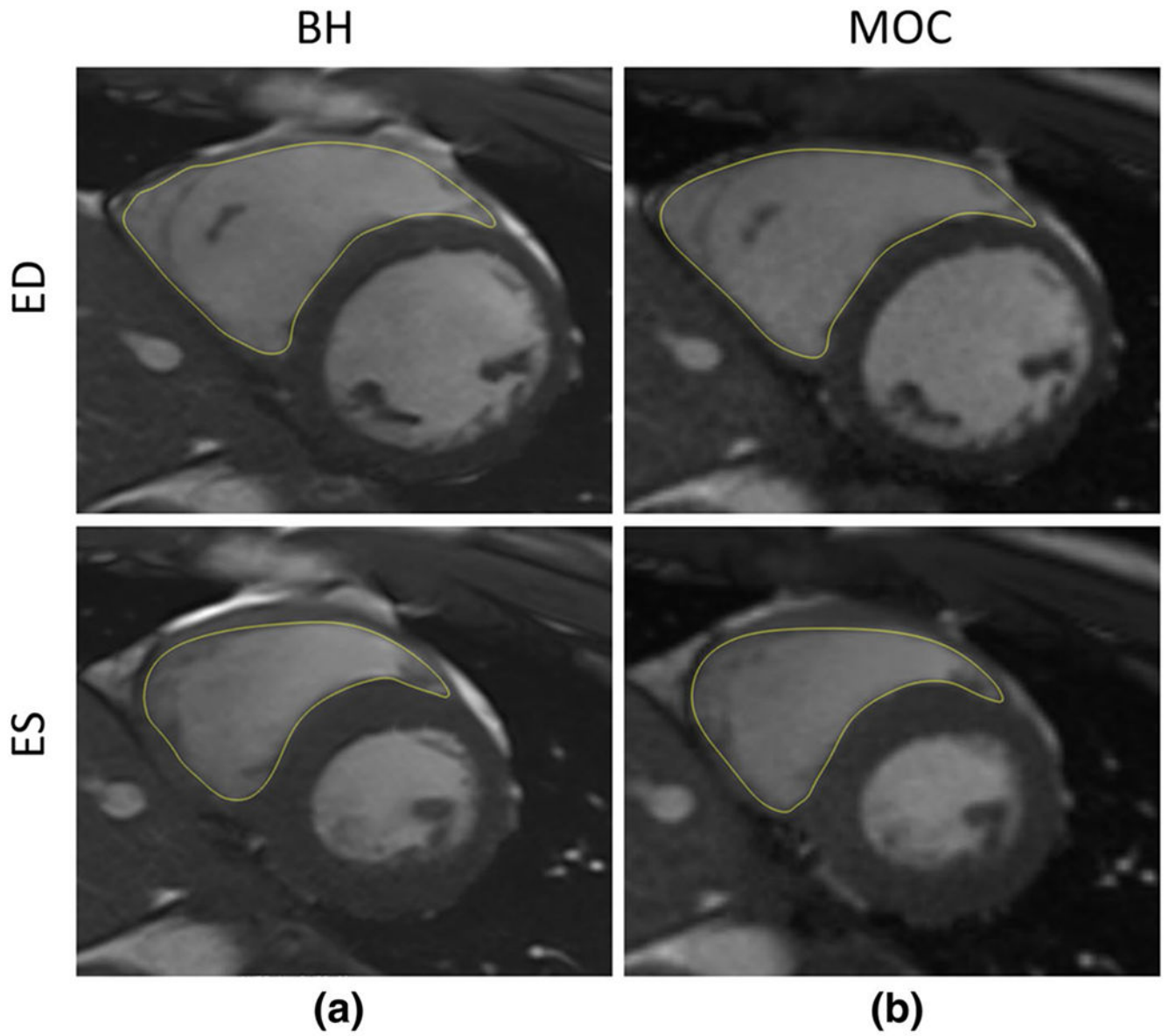


**Fig. 1.** Representative mid-ventricular end-diastolic (ED) and end-systolic (ES) images with endocardial and epicardial contour tracings for each acquisition type: **a** breath-held bSSFP, **b** retrospective motion corrected re-binning

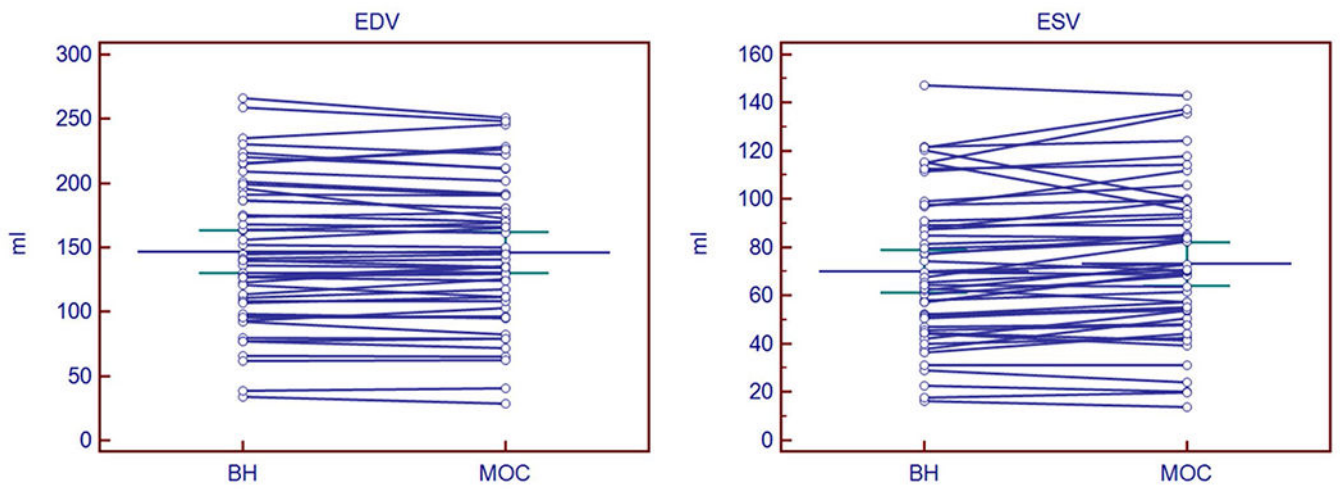


**Fig. 2.** Measured left ventricular end-diastolic volume (EDV) and end-systolic volume (ESV) for both acquisition sequences. Bars indicate mean  $\pm$  95% confidence intervals. *BH* breath-held bSSFP, *MOC* retrospective motion corrected re-binning

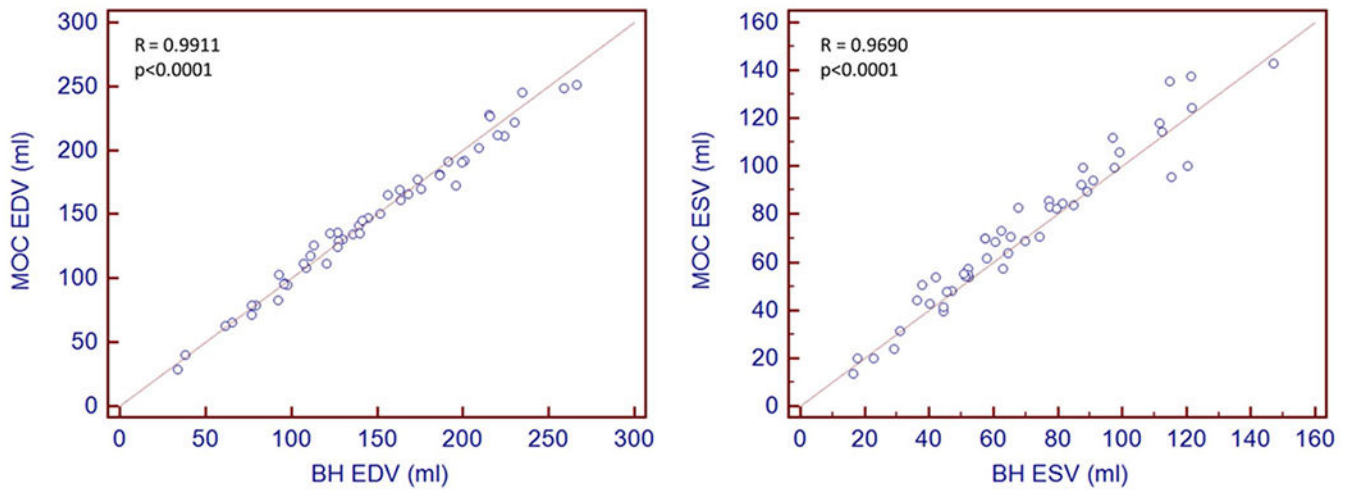


**Fig. 3.** Pearson correlation plots of volumetric quantification for retrospective motion corrected re-binning compared to the gold-standard breath-held SSFP for right ventricular end-diastolic volume (EDV) and end-systolic volume (ESV). *BH* breath-held SSFP, *MOC* retrospective motion corrected re-binning

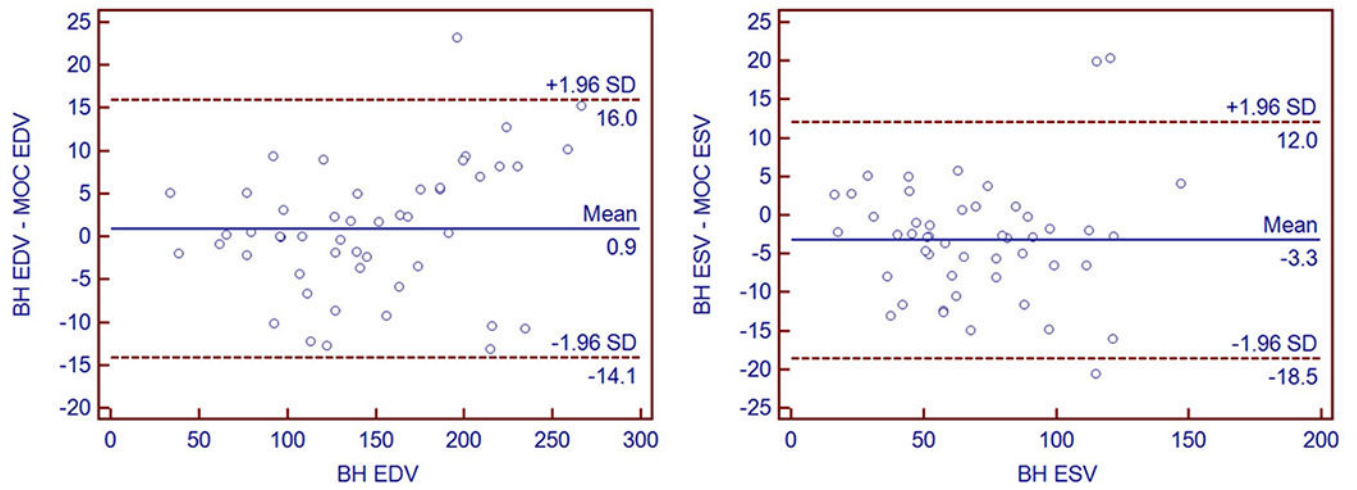


**Fig. 4.** Bland–Altman plots of right ventricular end-diastolic volume (EDV) and end-systolic volume (ESV) performed by the primary observer for re-binning compared to the clinical gold-standard of breath-held bSSFP. Measurement differences on y-axis are plotted against gold-standard BH measurement on x-axis. *BH* breath-held bSSFP, *MOC* retrospective motion corrected re-binning

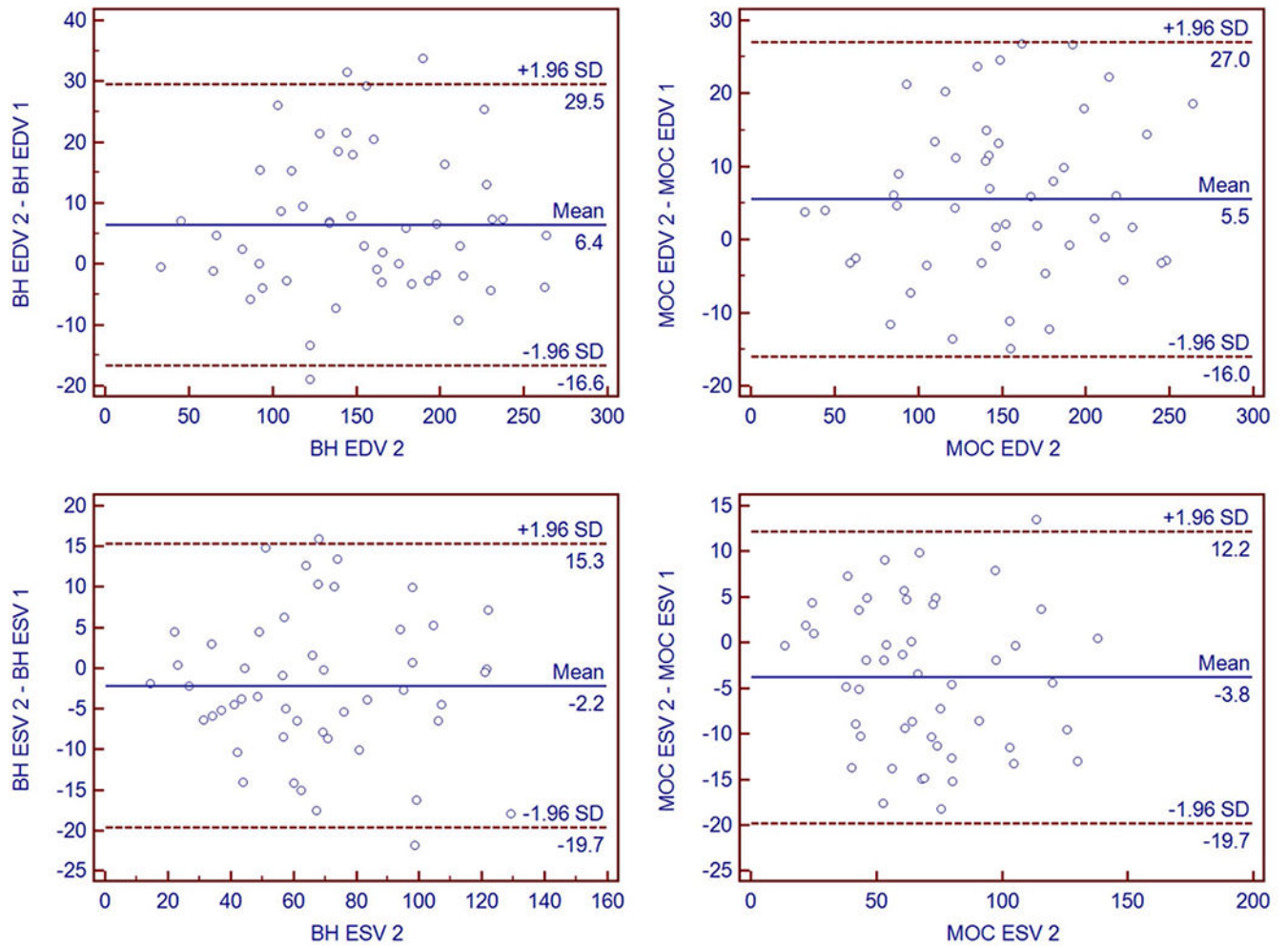


**Fig. 5.** Bland–Altman plots of right ventricular end-diastolic volume (EDV) and end-systolic volume (ESV) performed by each of two observers (Obs 1 and Obs 2) respectively for breath-held bSSFP and retrospective motion corrected re-binning image acquisitions. *BH* breath-held bSSFP, *MOC*retrospective motion corrected re-binning

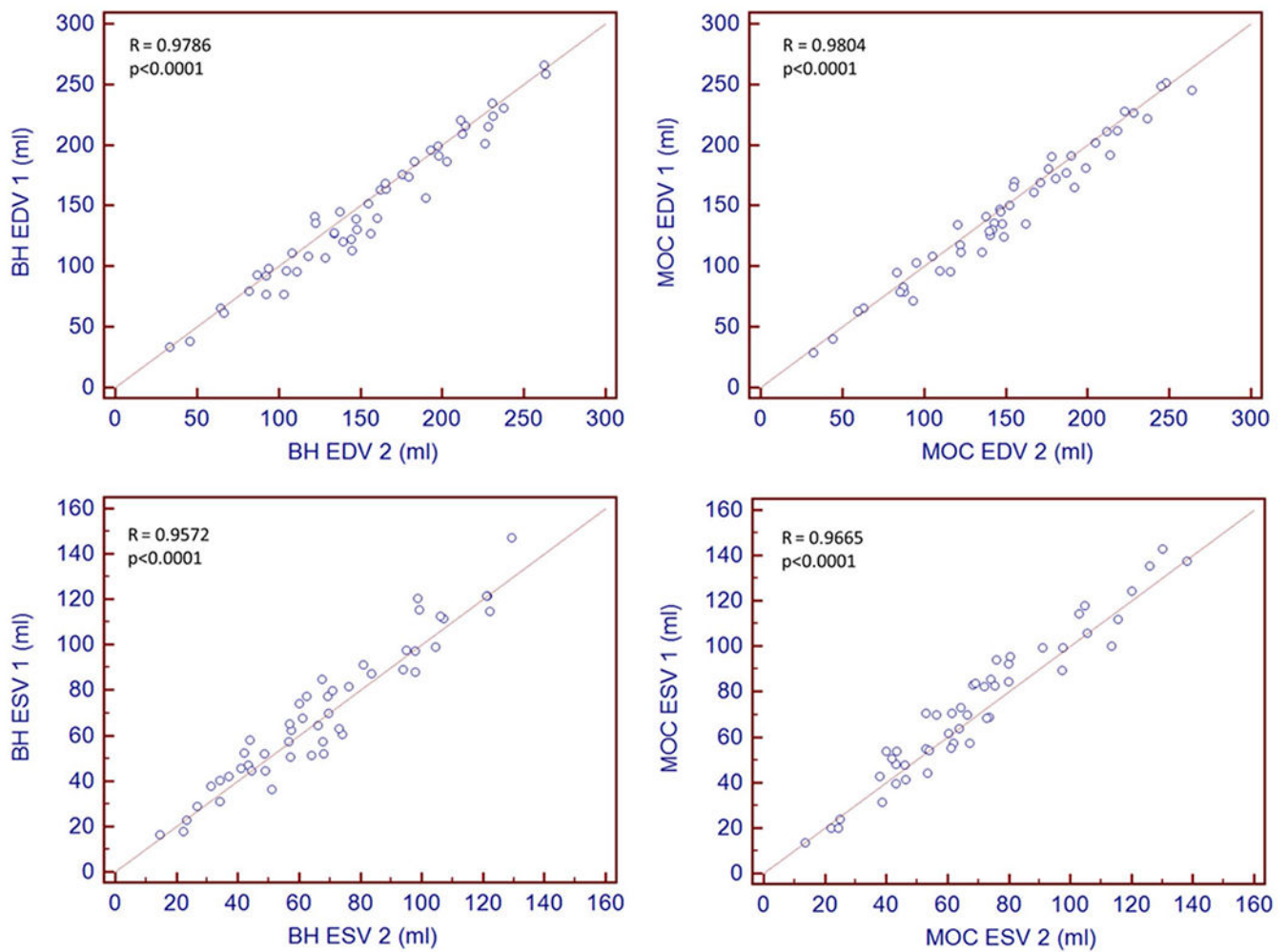


**Fig. 6.** Pearson correlation plots of volumetric quantification between two observers for both retrospective motion corrected re-binning compared and the gold-standard breath-held bSSFP with respect to right ventricular end-diastolic volume (EDV) and end-systolic volume (ESV). *BH* breath-held bSSFP, *MOC* retrospective motion corrected re-binning



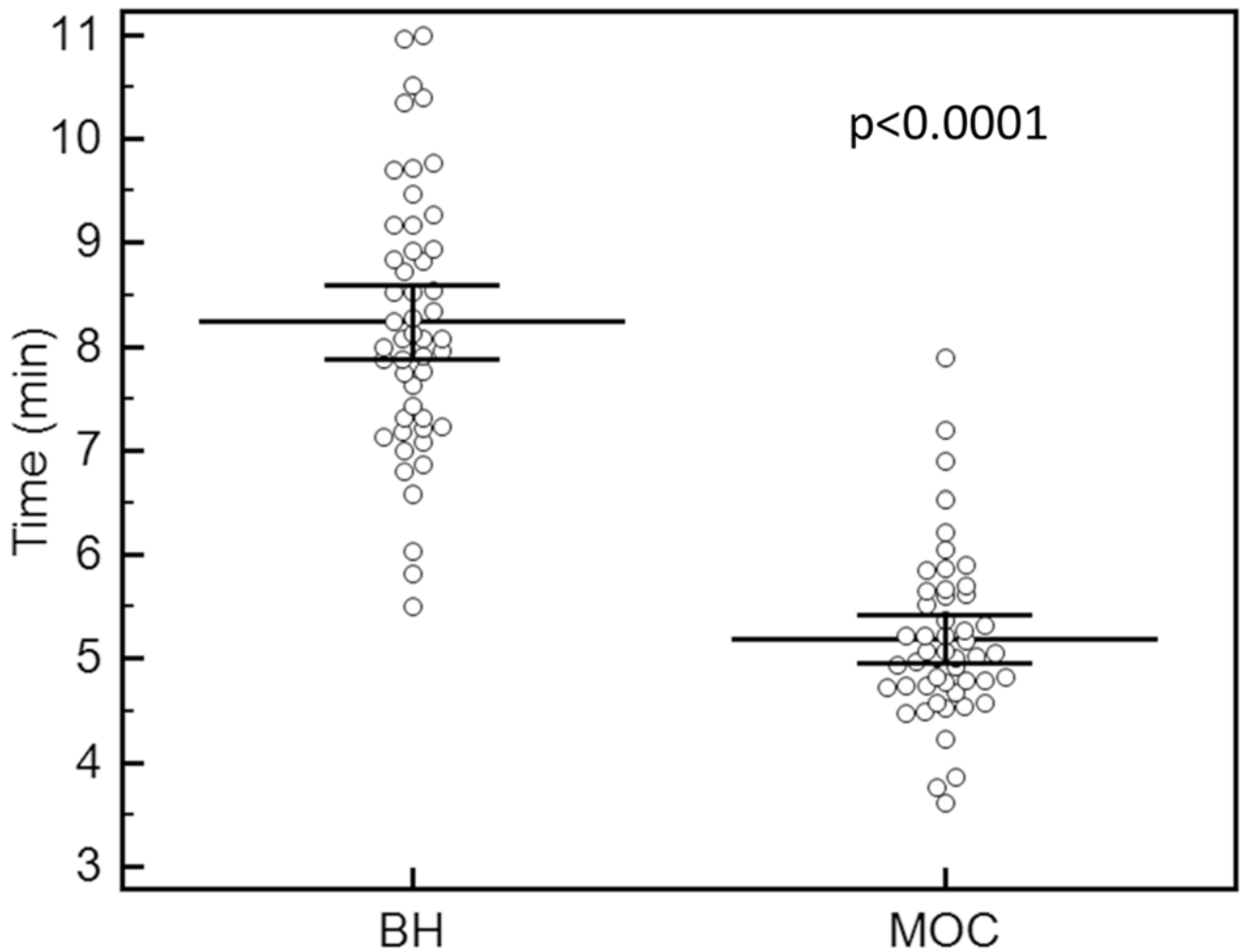


**Fig. 7.** Total image acquisition and reconstruction time in minutes for breath-held bSSFP and retrospective motion corrected re-binning image sequences. Lines indicate mean  $\pm$  95% confidence intervals. *BH* breath-held bSSFP, *MOC* retrospective motion corrected re-binning. Figure modified from Fig. 8 in Cross et al. [10] and used with permission from the author

**Table 1**

Summary of sequence parameters

	Infant ( <i>n</i> = 1)			Child ( <i>n</i> = 6)			Teenage/adult ( <i>n</i> = 43)		
	BH	MOC		BH	MOC		BH	MOC	
RFOV (mm)	220 × 165	220 × 165		270 × 202	270 × 202		360 × 270	360 × 270	
Matrix	192 × 144	192 × 144		208 × 156	208 × 156		256 × 192	256 × 192	
Slice thickness (mm)	4	4		6	6		8	8	
Gap (%)	0	0		33	33		25	25	
Echo time (ms)	1.12	1.21		1.13	1.22		1.1	1.19	
Echo spacing(ms)	2.9	2.9		2.9	2.5		2.8	2.8	
Number of segments	7	36 <sup>a</sup>		9	39 <sup>a</sup>		11	48 <sup>a</sup>	
Flip angle (deg)	50	50		50	50		50	50	
Acceleration factor	2	4		2	4		2	4	

<sup>a</sup>MOC images are re-binned on a higher temporal resolution.

RFOV = rectangular field of view with phase encoding direction 75% of frequency encoding direction

**Table 2**

Summary of Bland–Altman and concordance correlation statistics comparing inter–observer variability of volume measurements for two image acquisition techniques for 49 subjects

Statistic	EDV		ESV	
	BH	MOC	BH	MOC
Bland–Altman (ml)				
Bias	6.4	5.5	-2.2	-3.8
SD of bias	11.8	10.9	8.9	8.1
Min limit (95%)	-16.6	-16	-19.7	-19.7
Max limit (95%)	29.5	27	15.3	12.2
Correlation				
Concordance correlation coefficient ( $\rho_c$ )	0.9721	0.9755	0.9529	0.9572
95% CI	0.9517–0.9840	0.9574–0.9860	0.9191–0.9728	0.9269–0.9750
Pearson correlation coefficient ( $\rho$ )	0.9786	0.9804	0.9572	0.9665
Bias correction factor ( $\alpha_b$ )	0.9934	0.9950	0.9955	0.9903